Journal of the European Ceramic Society 20 (2000) 267–275

Powder characteristics, sintering behavior and microstructure of sol–gel derived ZTA composites

D. Doni Jayaseelan [a,*], D. Amutha Rani [b], Tadahiro Nishikawa [a], Hideo Awaji [a], F.D. Gnanam [b]

[a] *Department of Materials Science and Engineering, Nagoya Institute of Technology, Gokiso-cho, Showa-ku, Nagoya 466 8555, Japan*
[b] *Ceramic Division, Department of Chemical Engineering, Anna University, Chennai 600 025, India*

Received 17 September 1998; received in revised form 25 May 1999; accepted 1 June 1999

Abstract

A series of alumina/zirconia composites of varying compositions of zirconia were prepared through the sol–gel technique. Precursors were calcined at different temperatures ranging from 300 to 1400°C and sintered at 1530°C for 3 h. Compacts made from the powder calcined at 950°C yielded density up to >99% of theoretical density by pressureless sintering. Pore size distribution and the densification behavior were explained with respect to calcination temperature. Microstructural analysis of the sintered compacts revealed the uniform distribution of the zirconia grains in the alumina matrix. It is also observed that the faceted intergranular zirconia grains are at the grain junctions and the corners of the alumina matrix. © 2000 Elsevier Science Ltd. All rights reserved.

Keywords: Al_2O_3; Sol–gel processes; Sintering; Microstructure-final; ZTA

1. Introduction

The densification of zirconia toughened alumina (ZTA) has been achieved mostly by HIPing in the temperature range from 1400 to 1650°C[1,2] or by pressureless sintering which is carried out at high temperatures above 1600°C. However, the sintering temperature of alumina/zirconia composites can be lowered when the latter phase could give rise to grain coalescence phenomena. Several methods of preparing the alumina/zirconia powders have been reported. The conventional methods involve either dry milling[3] or wet milling[4] the mixture of available alumina and zirconia powders. However, an inhomogeneous mixing in terms of particle spacing and non-uniform ceramic microstructure cannot be avoided in this conventional approach. A further modification of this approach has involved using an aqueous slurry containing alumina and a selected zirconium salt for spray drying.[5] Aksay et al.[6] reported a new approach in which the particles of alumina and zirconia were mutually dispersed by controlling the pH of the aqueous medium from 2 to 3.5; the slurry thus produced was slip casted through gypsum mold to form the green composite bodies. This approach was modified by Lange et al.[7] who dispersed alumina and zirconia particles separately in the aqueous medium of pH = 2 and collected all particles smaller than 1 μm separately from each suspension by pH controlling sedimentation process.

Hence, it is worth mentioning here that the sinterability of ZTA composite is dependent on the powder processing route.[8] The concept of simultaneous sintering and phase transformation has been an alternative route for the preparation of alumina ceramics.[9] A drastic decrease in the densification rate has been observed upon the transformation from transitional aluminas to α-alumina, because the transformation to α-alumina is a nucleation and growth controlled process. Hence, one could obtain the microstructure after the alumina phase transformation that provides a better opportunity for low temperature pressureless sintering and optimum grain growth. The densification behavior can also be improved either by seeding the sol by α-alumina[10,11] or by suitably adjusting the calcination temperatures.[12–14] Hence, the objective of this present work is to study the

* Corresponding author. Tel.: +81-52-735-5287; fax: +81-52-735-5294.
E-mail address: doni@mse.nitech.ac.jp (D.D. Jayaseelan).

0955-2219/00/$ - see front matter © 2000 Elsevier Science Ltd. All rights reserved.
PII: S0955-2219(99)00165-X

influence of processing parameters on powder characteristics, sintering behavior and microstructure of the alumina/zirconia composites and to optimize the conditions to sinter the alumina/zirconia composites by pressureless sintering at relatively low temperature.

2. Powder processing

Fig. 1 shows the typical flow chart of the processing of alumina/zirconia composites. The procedure involves the following steps: preparation of stable (hydrous) boehmite and oxalate (zirconyl oxalate, cerium zirconyl oxalate and yttrium zirconyl oxalate) sols; mixing the sols in proper ratio to obtain the final precursor of desired composition and finally stabilizing the mixed sol. Three series of alumina/zirconia composites with (i) unstabilized zirconia, (ii) 12 mol% ceria-stabilized zirconia and (iii) 3 mol% yttria-stabilized zirconia of varying amounts (5, 10, 15, 20 and 25 vol%) of zirconia are considered for the present work.

The two sols were mixed in the proper ratio to have a desired composition and stirred vigorously for homogeneous mixing at room temperature for a few hours. The pH of the composite sol was maintained at the pH range of 3–3.5. After stabilizing the mixed sol, it was allowed to form a gel at room temperature and then oven dried at 110°C. The dried gel was repeatedly washed with alcohol and freeze dried. The freeze-dried precursors were again oven dried at 110°C to remove any residual moisture. The amorphous precursors were calcined at different temperatures ranging from 300 to 1400°C for 3 h to examine the influence of the calcination temperature on the crystallization behavior of alumina and zirconia composites.

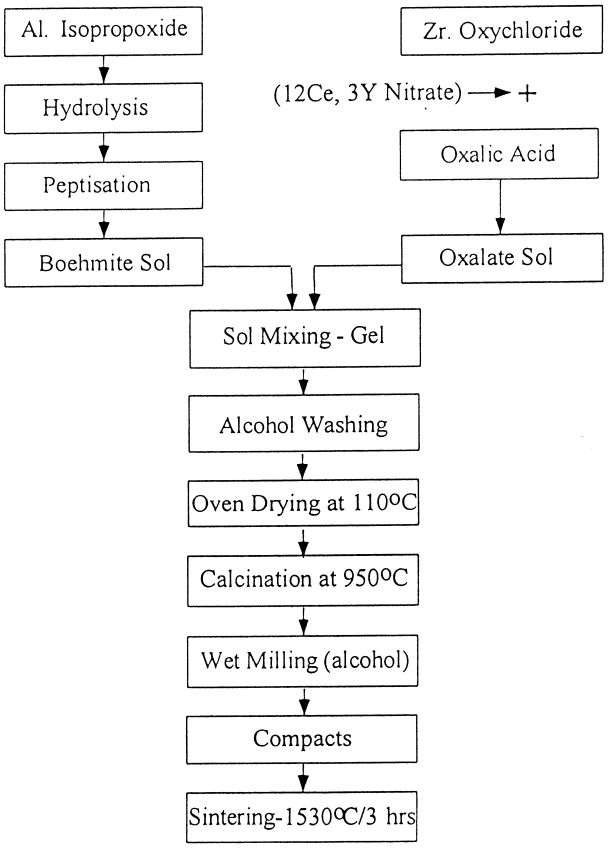

Fig. 1. Flow chart for the processing of alumina/zirconia composites.

The precursors calcined at different temperatures were wet ball milled in alcohol for 12 h. The charge to media ratio 1:2 was kept constant for all the composition. The wet milled powders were then oven dried at 110°C for 24 h. The dried powders were uniaxially pressed into pellets of dimension 15 × 10 mm at 200 MPa and oven dried at 110°C. The dried compacts were heated to 600°C and kept for 3 h to burn out any organic residue and then sintered to a maximum temperature of 1530°C for 3 h.

3. Characterization

Thermal behavior of the as dried and the alcohol washed precursors and the chemistry of the precursors calcined at different temperatures were studied by differential thermal analysis (DTA) and infrared (IR) analysis, respectively. The phase formation of the powders was determined by X-ray diffractometry using Cu-K_α as the radiation source and Ni as the filter. The crystallite size was determined from X-ray line broadening using the Sherrer's equation,

$$D = \frac{0.9\lambda}{\beta \cos\theta} \quad (1)$$

where D is the crystallite size, λ is the wavelength of the radiation, θ is the Bragg's angle and β is the full width at half maximum.

Particle size analysis of the as dried and the calcined powders was carried out by laser diffraction particle size analyzer. The pore structures of the as dried and the calcined powders were derived from the shape of the N_2 adsorption/desorption isotherm measured at liquid N_2 temperature after degassing at 300°C for 1 h. The specific surface area for all the calcined powders was determined by BET method. The particle morphology of the freeze-dried calcined powder was observed using SEM. Bulk density of the sintered samples was measured using Archimede's method. Theoretical density of all the composites was calculated using the rule of mixtures. The sintered samples were lapped and then polished to 1 μm using diamond paste. The polished samples were thermally etched at 1450°C for 30 min. The microstructure of the samples were observed using SEM.

4. Results and discussion

4.1. Effect of calcination temperature

It is well known that the calcination temperature has a strong influence on the morphology of the powders and their sintering behavior.[13–15] The final sintering temperature of ZTA is related to the amount of densification of the transition alumina aggregates during calcination and sintering and the microstructural changes that occur during calcination. Porosity persists during subsequent alumina phase transformation, thus giving rise to a microstructure, which densifies only at a higher temperature. The higher sintering temperature is most likely to be caused by the presence of more irregularly shaped transitional alumina particles. Table 1 summarizes the physical properties of the alumina/zirconia precursors calcined at different temperatures. In this present study, it is demonstrated that by means of a proper selection of the calcination temperature and pore structure of gel derived alumina/zirconia precursor, a dense microstructure after sintering can be obtained.

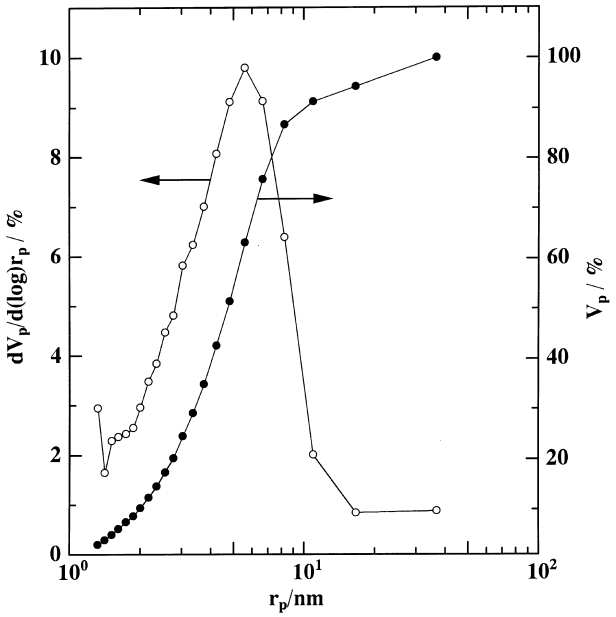

Fig. 2. Pore size distribution of alumina/15 vol% (3Y) zirconia precursors calcined at 950°C for 3 h.

4.1.1. Pore structure and pore size distribution

Fig. 2 gives the pore size distribution showing that the mean pore radius was approximately 4.8 nm. The specific surface area was determined to be 85 $m^2\ g^{-1}$ by the BET method and was quite higher than the powders calcined at other temperatures. Fig. 3 indicates the N_2 adsorption–desorption curves of alumina/15 vol% (3Y) zirconia precursors calcined at 950°C. The shape of the isotherm shows the characteristic behavior of the structure of powder, which is composed of an assembly of particles with large open packing. The hysteresis loop in the relative pressure of 0.5–0.9 typically results from wedge-shaped capillaries with a closed edge at the narrower side. This type of hysteresis has also been observed for the powders calcined at low temperatures (< 950°C) and thus, it is concluded that it is formed from the intra-aggregate pore structure. A minute hysteresis seen for powder calcined at 1250°C (Fig. 4) indicates the micro- and meso-pore structures with pore sizes in the nm region. However, for the powder calcined at 1250°C, the hysteresis loop in the relative pressure range from 0.4 to 0.8 is of the A-type of De-Boer's classification of isotherms[16] and corresponds to open capillaries with wide openings and narrow short necks and obviously results from inter-aggregate pores. Powders calcined at temperatures > 1000°C have only A-type inter-aggregate pores suggesting that the aggregates densified during calcination at a temperature > 1000°C. From the pore volume measurements, it is clear that the powders calcined at 950°C are of porous nature. It is also observed from the IR study that the precursor contains hydroxides of alumina up to 600°C and hence calcination

Table 1
Powder characteristics of alumina/zirconia precursors

ZrO_2 (3Y) vol%	Calcination temperature (°C)	Specific surface area (m^2/g)	Mean particle size (d_{50}) (μm)	Average pore radius (nm)	Crystallite size (nm)		Identified phases[a]
					Zirconia	Alumina	
5	300	257	3.9	–	–	–	γ
	950	85	1.8	–	–	–	δ, θ, α, t
	1250	1	2.8	–	4	7	α, t
15	300	272	6.3	1	–	–	γ
	950	89	4	4.8	2	–	δ, θ, α, t
	1250	2.7	4	3.5	4	5	α, t
25	300	285	7.2	–	–	–	γ
	950	95	4	–	2	4	δ, θ, α, t
	1250	3.4	4	-	4	5	α, t

[a] ν δ, θ, α, phases of alumina; t-phases of zirconia.

at 950°C leads to the evolution of these hydroxides, which in turn generate pores. Hence, during wet milling these highly porous powders have been crushed into fine particles (Table 1), which is desirable for the low temperature sintering of the composites.

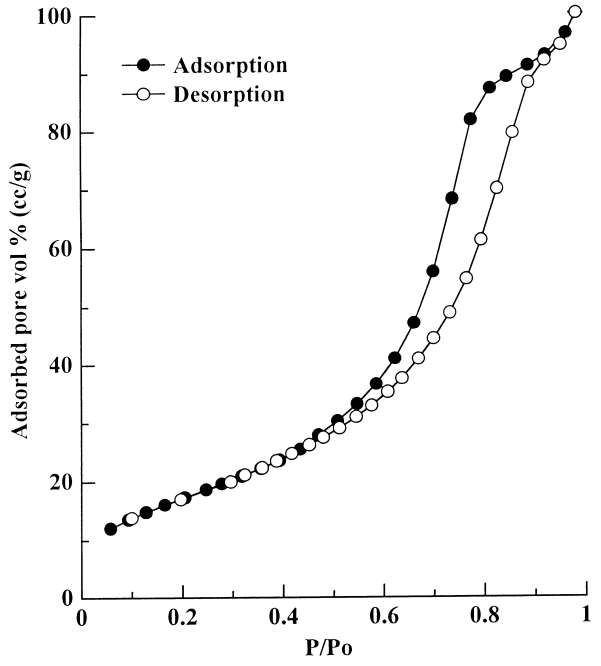

Fig. 3. Nitrogen adsorption/desorption isotherms of alumina/15 vol% (3Y) zirconia precursors calcined at 950°C for 3 h.

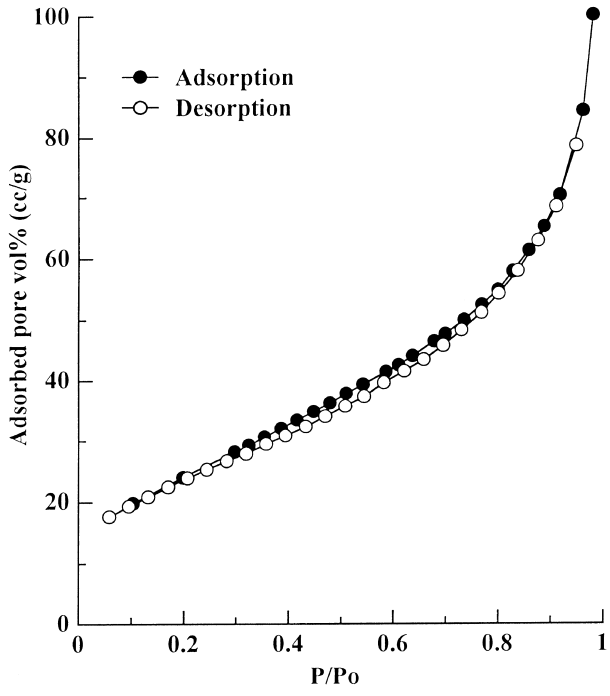

Fig. 4. Nitrogen adsorption/desorption of alumina/15 vol% (3Y) zirconia precursors calcined at 1250°C for 3 h.

4.1.2. X-ray diffraction analysis

The powders were characterized for their formation of phases using the XRD technique. Fig. 5 shows the XRD patterns of alumina/15 vol% (3Y) zirconia precursors calcined at different temperatures. The t-phase of zirconia and δ-phase of alumina were the first crystalline phases appeared after calcination at low temperatures. Above 600°C, δ-alumina was prominent but transformed into θ-alumina at 950°C. The t-phase of zirconia peaks were sharper than the δ-alumina peaks, indicating the formation of well crystallized t-zirconia. However, after calcination at 1250°C, θ-alumina completely transformed to α-alumina.

4.1.3. IR analysis

Fig. 6 shows the IR spectrum of the evolution of gel precursor to crystallize during calcination at different temperatures. The spectrum of low temperature (300°C) calcined powder produces a sharp band at about 1072 cm^{-1}, which corresponds to the absorption of Al–OH groups. The absorption band at 1639 cm^{-1} is ascribed to O–H bending vibrations and the bands in the region 1000–400 cm^{-1} to Al–O vibrations. The OH and Al–O vibrations are characteristics of pseudo boehmite. When calcined above 600°C, all these absorption peaks disappear and the broad band in the region 1000–400 cm^{-1} corresponds to Al–O vibrational modes. However, the O–H vibrations of adhesive water are present. The 1250°C

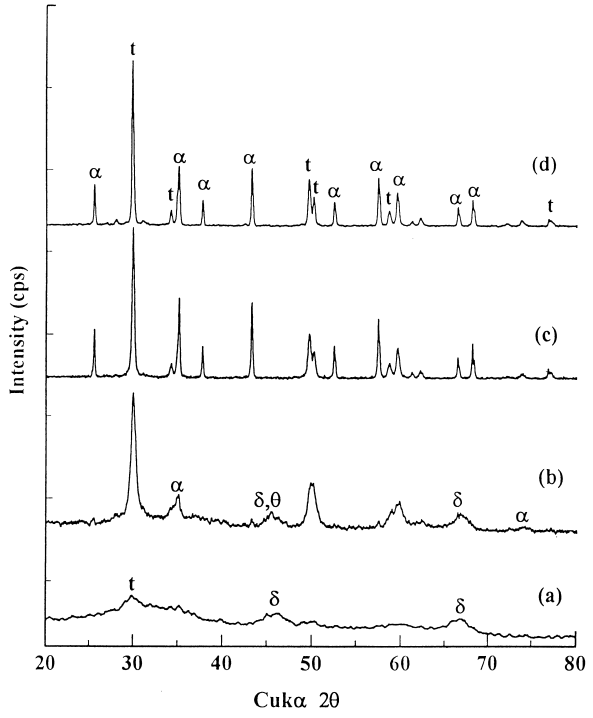

Fig. 5. XRD patterns of alumina/15 vol% (3Y) zirconia precursors calcined at different temperatures: (a) 600°C; (b) 950°C; (c) 1250°C; (d) 1400°C.

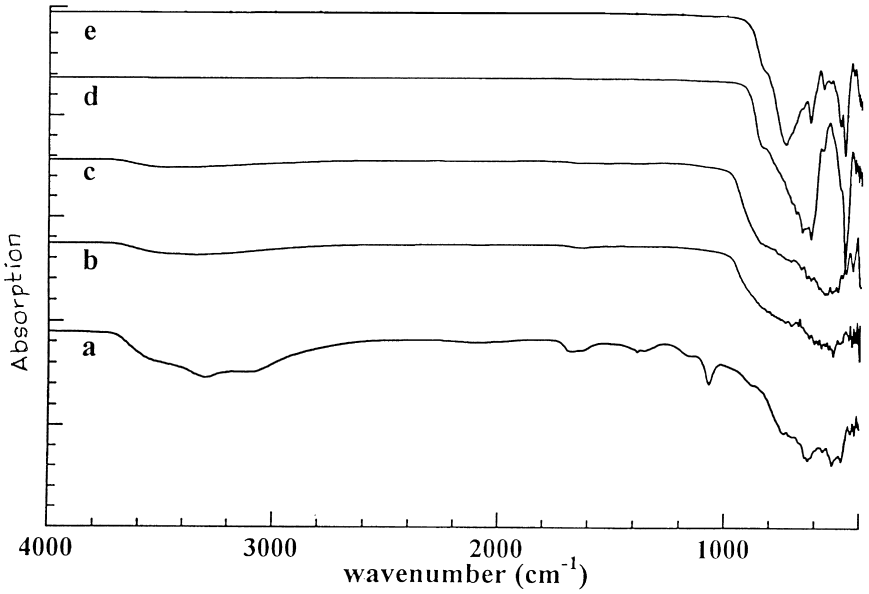

Fig. 6. IR patterns of alumina/15 vol% (3Y) zirconia precursors calcined at different temperatures: (a) 300°C; (b) 600°C; (c) 950°C; (d) 1250°C; (e) 1400°C.

treatment leads to the conversion of all hydroxides into oxides, as is evident from the disappearance of Al–OH vibration.

4.1.4. Density studies

Fig. 7 shows the sintered density of the alumina/15 vol% (3Y) zirconia composites with respect to their calcination temperature. It is observed that the sintered density of the compacts increases with increase in calcination temperature and reaches a maximum value at 950°C. Due to the presence of higher amount of hydrates, weight loss has been observed after sintering for powder calcined at low temperatures. These hydrated molecules dissociate during sintering and will leave the residual pores. These pores are very difficult to remove during the final stage of sintering. These factors are responsible for the low sintered density for the powder calcined at low temperatures. The compacts prepared from powder calcined at 1250°C also contains α-alumina and cannot be sintered to a high density within 3 h at 1530°C (Fig. 6). Also it cannot be ruled out that the calcination at a temperature as high as 1200°C for 2 h resulted in α-alumina nuclei. Although, based on the difference in calcination temperature, a different amount of α-alumina nuclei should be expected, the densification behavior of compacts prepared from powder calcined at either 1100 or 1250°C did not show much difference. The influence of possible α-alumina nuclei can thus be left out. Nevertheless, the decrease in sintered density above 950°C is due to the growth of grains with irregularly shaped pore structure. It is observed from Table 1 that the powder calcined at 950°C contains transitional phases of alumina. This microstructure development with phase transformation is obviously the most important sintering step for the densification of transitional alumina-containing composites. The shorter diffusion length and higher surface curvature of the submicron sized powder help to lower the sintering temperature and minimize coarsening. In addition, the pore structure developed upon calcination plays a vital role in further sintering. Therefore, the optimal calcination for densification of alumina/zirconia composite could be 950°C for 3 h. Hori et al.[17] also reported an optimal calcination temperature between 800 and 1000°C. The ZTA specimen prepared by them through the CVD method yielded very high density. Balasubramanian et al.[18] have also reported that the precursors calcined at 950°C for 3 h show better densification behavior. However, only 90% of TD has been obtained, when the powder compact has been sintered at 1630°C for 3 h.

4.2. Effect of zirconia content

It is clear that the formation of α-alumina takes place from the transitional aluminas (Fig. 5). The hydroxides of aluminium and its derivatives are dehydrated to form transitional aluminas with changes in pore structure to accommodate densification.[19,20] This transformation is possible since the transitional aluminas differ from each other only in the degree of ordering of the oxygen lattice. The formation of α-alumina from transitional aluminas involves the rearrangement of the oxygen lattice from a more or less distorted cubic array to a hexagonal close packed structure. After this transformation, the cations occupy the octahedral sites and there is an

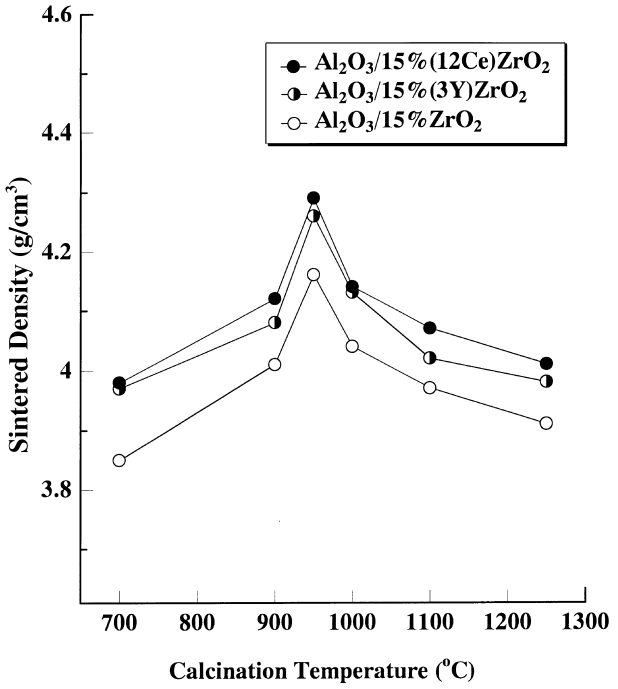

Fig. 7. Sintered density of alumina/15 vol% (3Y) zirconia composites sintered at 1530°C for 3 h with respect to calcination temperature.

increasing ordering of the cation vacancies. As α-alumina forms by a nucleation and growth process, spherical colonies of α-alumina nucleate in a porous matrix of transitional aluminas and grow gradually via the coarsening process. Higher amounts of zirconia can be dissolved in transitional aluminas than in α-alumina because of the cubic spinel structure with a considerable number of defects and disorder.[19] During the transformation of α-alumina, the zirconia comes out of the cubic lattice sites and enters the interstitial and vacant lattice sites causing expansion of the lattice along the a-axis. These zirconium ions preferably exert dragging force on the diffusion of aluminium ions[4,21] and hence the transformation to α-alumina occurs at higher temperatures in the presence of zirconia.

On the other hand, the constraints imposed by the surrounding alumina grains influence the zirconia transformation. Alumina matrix with high elastic modulus and thermal expansion coefficient restricts the expansion of zirconia occurring during $t \rightarrow m$ transformation and reduces the transformation temperature. Zirconia present in the composite is, therefore, retained in the tetragonal form because of its fine size and constraints imposed by the alumina grains. The t-phase of zirconia in the ZTA composites was stable up to 1400°C. Due to the presence of zirconia, the complete conversion of α-alumina occurs at a higher temperature than usual temperature, which occurs around 1100°C,[12] which is evident from an exothermic peak 1230°C in Fig. 8. From Fig. 8, one can observe that the α-alumina phase transformation is shifted from 1230 to 1270°C due to the increase in the % of zirconia content.

Fig. 9 shows the sintered density of the samples of the three series of composites calcined at 950°C for 3 h and sintered at 1530°C for 3 h, with respect to zirconia content. Though, the alumina phase transformation in powder is shifted from 1230 to 1270°C, the presence of zirconia, however, did not affect the densification behavior of the composites. The sintered compacts yield density up to >99% of the TD. It is observed from Fig. 9 that the relative density of the sintered composite containing unstabilized zirconia decreases with respect to zirconia content, unlike ceria and yttria stabilized

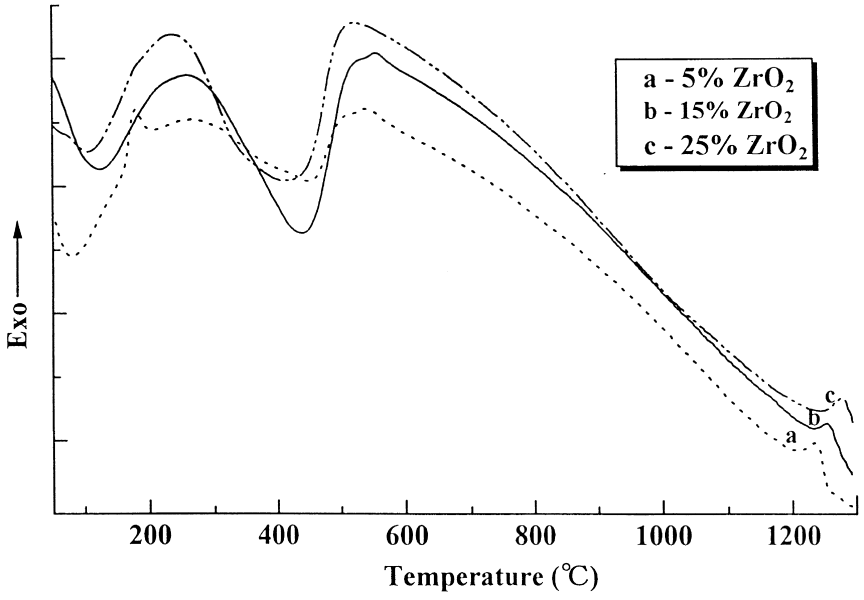

Fig. 8. DTA curves of the alumina/15 vol% (3Y) zirconia precursors with respect to zirconia content.

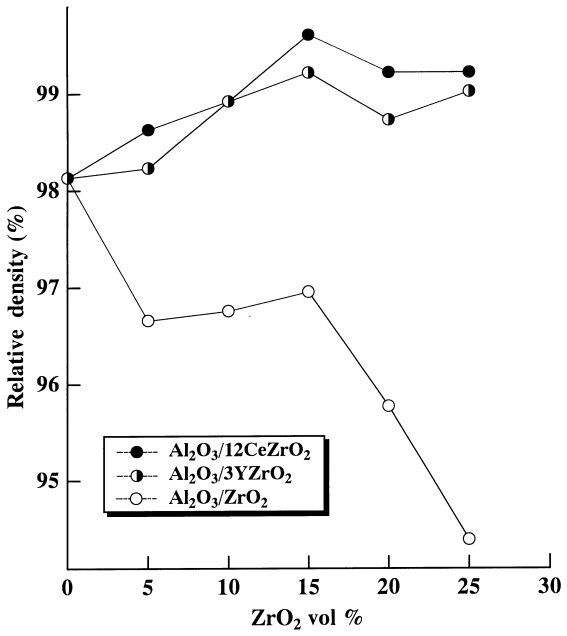

Fig. 9. Relative density of the alumina/zirconia composites sintered at 1530°C for 3 h.

zirconia containing composites. This is due to the decrease of t-phase with increase in the zirconia content for the unstabilized zirconia. This $t \rightarrow m$ phase transformation of zirconia causes volume expansion leading to a decrease in the relative density of the composite.

5. Microstructure

Fig. 10a shows the microstructure of the powder compact calcined at 1250°C for 3 h, compacted at 200 MPa uniaxially and sintered at 1530°C for 3 h. The large void is attributed to the differential sintering of the alumina and zirconia phases and due to the excessive calcination. Hence, the decrease in the sintered density could be due to the aggregate and pore structure, which inhibit the sintering of ZTA compact. Fig. 10b shows the typical microstructure of polished and thermally etched specimens of alumina/25% (3Y) zirconia composite calcined at 950°C for 3 h and sintered at 1530°C. It is observed that the compact has attained full densification. It is also observed that from the back scattered

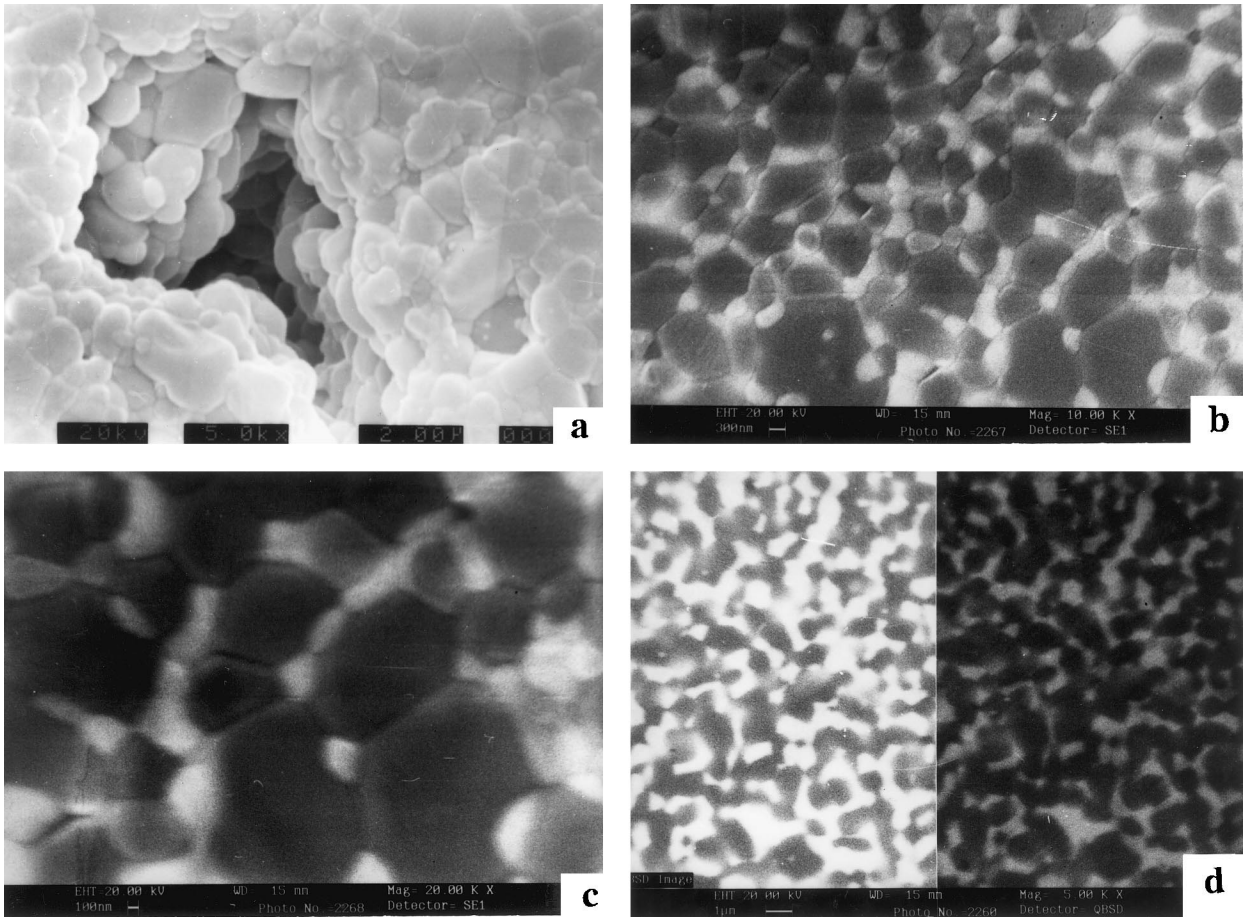

Fig. 10. (a) Microstructure of the sintered alumina/zirconia composite calcined at 1250°C. (b) Microstructure of the sintered alumina/zirconia composite calcined at 950°C. (c) Microstructure of the sintered alumina/zirconia composite calcined at 950°C. (d) SE and BS images of the sintered alumina/zirconia composites calcined at 950°C.

(BS) image (Fig. 10d), the small zirconia grains are located between large grains revealing the uniform dispersion of zirconia grains in the alumina matrix. It is believed that the zirconia grains, which are primarily located at the triple junctions must be due to the strong self-diffusion of zirconia although some small zirconia grains become relocated within some alumina grains and had a spherical geometry. This phenomenon can be suggested to occur by the growth of alumina grains, constrained by relatively few zirconia grains into a single large grain which then 'swallowed up' surrounding alumina and zirconia grains. Lange and Hirlinger[21] also observed various drag/breakaway configurations including zirconia grains near the three-grain junctions and at two-grain boundaries (Fig. 10c). It is also observed from Fig. 10c that two kinds of zirconia grains exist in the ZTA composite, namely (i) faceted intergranular zirconia grains (mostly at the grain corners) and (ii) spherical intragranular zirconia grains. The large intergranular grains may be related to the faster coarsening rate.

During sintering, finely dispersed zirconia particles located at grain boundaries retard the motion of the alumina grain boundaries (inhibit grain growth). However, these zirconia particles eventually coalesce with each other, are located at grain junctions (i.e. little effect on suppressing grain growth) and are responsible for a grain boundary pinning effect. However, the addition of 25 vol% of zirconia still shows abnormal grains. The large grains found in the sample are still due to non-uniform distribution of zirconia grains, which are not sufficient to hinder the growth of every alumina grain. As most zirconia grains are located at triple junctions and at grain boundaries of alumina, coarsening of zirconia grains are controlled by the coalescence. It is also clear from Fig. 10c (secondary electron image) that the volume fraction of zirconia influences the spatial distribution of zirconia grains and high volume fraction of zirconia causes the zirconia to be less isolated and more continuous and interconnected.

6. Conclusion

Alumina/zirconia composites containing various types of zirconia with varying compositions were prepared through the sol–gel technique. The alcohol washed powders showed better performance and the conversion temperature of transitional aluminas to α-alumina was lowered from 1230 to 1170°C. The present experimental results showed that the powders calcined at 950°C had better textural properties than the other low and high temperature calcined powders. Samples calcined at 950°C for 3 h and pressureless sintered at 1530°C for 3 h, yielded density up to $>99\%$ of the TD. The SEM micrograph of the alcohol-washed and freeze dried powder was observed to have spherical morphology. The microstructure of the polished and the thermally etched samples revealed that the zirconia grains were uniformly distributed in the alumina matrix. Most of the grains were located at the junctions of the alumina grains and the grain boundaries, which revealed the intergranular nature of the zirconia grains. Very few grains were located within the alumina grains, possessing the intragranular type. As most of the zirconia grains were placed at the grain junctions, the zirconia grains pinned down the motion of the alumina grains.

References

1. Hori, S., Somiya, H. Y. and Kaji, H., Change of tetragonal-zirconia content in zirconia-toughened alumina by host isostatic pressing. *J. Mat. Sci. Letts*, 1988, **3**, 242–244.
2. Bhattacharya, S. and Jakus, K. S., Hot pressing of annular alumina–zirconia composites. *J. Am. Ceram. Soc.*, 1998, **81**, 460–464.
3. Murase, Y., Kato, E. and Daimon, K., Stability of ZrO_2 phases in ultrafine ZrO_2–Al_2O_3 mixtures. *J. Am. Ceram. Soc.*, 1986, **69**, 83–87.
4. Green, D. J., Critical microstructures for microcracking in Al_2O_3–ZrO_2 composites. *J. Am. Ceram. Soc.*, 1982, **65**, 610–614.
5. Ruhle, M., Heuer, A. H. and Claussen, N., Transformation and microcrack toughening as complementary processes in zirconia-toughened alumina. *J. Am. Ceram. Soc.*, 1986, **69**, 195–197.
6. Aksya, I. A., Lange, F. F. and Davis, B. I., Uniformity of Al_2O_3/ZrO_2 composites by colloidal filtration. *J. Am. Ceram. Soc.*, 1983, **66**, 190–192.
7. Lange, F. F., Yamaguchi, T. and Davis, B. I., Effect of ZrO_2 inclusions on the sinterability of Al_2O_3. *J. Am. Ceram. Soc.*, 1988, **71**, 446–448.
8. Koh, S. C. H., Air, K. A. and McPherson, R., Science and technology of zirconia. III. In *Advances in Ceramics*, ed. S. Somiya, N. Yamamoto and H. Hanagida. J. Am. Ceram. Soc., Westerville, OH, 1988, pp. 293–307.
9. Badkar, P. A. and Bailey, J. E., The mechanism of simultaneous sintering and phase transformation in alumina. *J. Mat. Sci.*, 1976, **11**, 1792–1806.
10. Srdic, V. and Radonjic, L., Interactions in the sol–gel processing of alumina/zirconia composites. *J. Euro. Ceram. Soc.*, 1994, **14**, 237–244.
11. Kumagai, M. and Messing, G. L., Enhanced densification of boehmite sol–gel by α-alumina seeding. *J. Am. Ceram. Soc.*, 1984, **60**, c230–c231.
12. Exter, P. D., Winnubst, L., Leuwerink, T. H. P. and Burgraaf, A. J., Effect of calcination on the sintering of gel-derived zirconia-toughened alumina. *J. Am. Ceram. Soc.*, 1994, **77**, 2376–2380.
13. Montanaro, L., Ferroni, L., Paglialico, S., Swain, M. V. and Bell, T. J., Influence of calcination temperature on the microstructure and mechanical properties of gel-derived and sintered 3 mol% Y-TZP material. *J. Am. Ceram. Soc.*, 1996, **79**, 1034–1040.
14. Jayaseelan, D. D., Nishikawa, T., Awaji, H. and Gnanam, F. D., Pressureless sintering of sol–gel derived alumina/zirconia composites. *Mat. Sci. Eng. A*, 1998, **256**, 265–270.
15. Kuo, J. and Bourell, D. L., Structural evolution during calcination of sol–gel synthesized alumina and alumina-8 vol% zirconia composites. *J. Mat. Sci.*, 1997, **32**, 2687–2692.
16. Boer, D. J. H., The shape of capillaries in the structure and properties of porous materials. In *Proc. of the 10th Symp. Colstone Res. Soc.*, ed. D. H. Everett and F. S. Stone. Butterworths Sci. Publ., Bristol, UK, 1958, pp. 68–94.
17. Hori, S., Yoshimura, M., Somiya, S. and Takanasaki, R., Al_2O_3–ZrO_2 ceramics prepared from CVD powders. In *Design of*

Advance in Ceramics 12, Science and Technology of ZrO_2 II. ed. N. Claussen, M. Ruhle and A. H. Heuer. Am. Ceram. Soc., 1991, Vol. 74, pp. 625–632.

18. Balasubramanian, M., Malhotra, S. K. and Gokularathnam, C. V., Influence of calcination temperature on the properties of spray dried alumina-zirconia composite powders. *J. Mat. Sci.*, 1995, **30**, 3515–3520.
19. Lippens, B. C. and Boer, D. J. H., Study of phase transformation during calcination of aluminium hydroxides by SAD. *Acta Crystall.*, 1964, **17**, 1312–1321.
20. Wilson, S. J., The dehydration of boehmite, γ-AlOOH to γ-Al_2O_3. *J. Sol. State Chem.*, 1979, **30**, 247–256.
21. Lange, F. F. and Hirlinger, M., Hinderance of grains growth in Al_2O_3 by ZrO_2 inclusions. *J. Am. Ceram. Soc.*, 1984, **67**, 164–168.